Conclusions. The conclusions that are independent of the source material are:

1. The $M_\nu = 0$ hypothesis is incompatible (statistically at a high confidence level) with our experimental data. This indicates that at least one neutrino has a non-zero mass.

2. $14 < M_{\tilde{\nu}_e} < 46$ eV at a 99% confidence level if $\tilde{\nu}_e$ is a mass eigenstate.

The conclusions that are dependent on the source material are:

3. If the final state spectrum of ^3He in the source corresponds effectively to the one final state spectrum*, then

$$14 < M_{\tilde{\nu}_e} < 26 \text{ eV at a 99\% confidence level} \qquad (16)$$

if $\tilde{\nu}_e$ is a mass eigenstate.

4. If the final state spectrum of ^3He corresponds effectively to the atomic tritium spectrum ($\omega_2 = 0.3$; $\Delta E_2 = 43$ eV), then

$$24 < M_{\tilde{\nu}_e} < 46 \text{ eV at a 99\% confidence level} \qquad (17)$$

For the time being we do not see any effects which could have essentially changed these limits.

---

*In a complex system (like valine) there may be numerous levels. However, if $\Delta E_i < R$ and $\sum \Delta E_i \leq R$, then the system will effectively be almost a one-level system (at FWHM, $R \simeq 54$ eV).

SOME PHENOMENOLOGICAL CONSIDERATIONS OF NEUTRINO OSCILLATIONS IN VACUUM AND MATTER

V. Barger
Physics Department, University of Wisconsin, Madison, WI 53706

ABSTRACT

Neutrino oscillation phenomena are reviewed, including indications from solar and reactor experiments, accelerator limits, CP violation tests, and deep mine possibilities for measuring vacuum oscillations and matter corrections.

INTRODUCTION

The weak interaction eigenstates of neutrinos ν_α (with $\alpha = e,\mu,\tau$) are related to the mass eigenstates ν_i (mass m_i with $i = 1,2,3$) by a unitary transformation

$$|\nu_\alpha\rangle = \sum_i U_{\alpha i}|\nu_i\rangle \ . \qquad (1)$$

For a ν_α state of momentum p, the time evolution is

$$|\nu_\alpha\rangle = \sum_i e^{-iE_i t} U_{\alpha i}|\nu_i\rangle = \sum_{i,\beta} e^{-iE_i t} U_{\alpha i}U^*_{\beta i}|\nu_\beta\rangle \ . \qquad (2)$$

At a distance $L \simeq t$ from a relativistic ν_α source, the $\nu_\alpha \to \nu_\beta$ transition probability is

$$P(\alpha\to\beta) = |\sum_i e^{-i\Delta_{in}} U_{\alpha i}U^*_{\beta i}|^2 \qquad (3)$$

where

$$\Delta_{in} = \frac{(m_i^2-m_n^2)L}{2E} = \frac{\delta m^2_{in}L}{2E} \ . \qquad (4)$$

In units $\delta m^2(eV^2)$, L(m), and E(MeV), $\Delta/2 = 1.27\delta m^2 L/E$. In the special case of oscillations involving two neutrinos only (e.g., ν_e,ν_μ), the mixing matrix is real

$$U = \begin{pmatrix} \cos\alpha & \sin\alpha \\ -\sin\alpha & \cos\alpha \end{pmatrix} \qquad (5)$$

and the transition probabilities are given by

$$\begin{aligned} P(e\to e) &= P(\mu\to\mu) = 1 - \sin^2 2\alpha \sin^2 \tfrac{1}{2}\Delta \\ P(e\to\mu) &= P(\mu\to e) = \sin^2 2\alpha \sin^2 \tfrac{1}{2}\Delta \ . \end{aligned} \qquad (6)$$

The sensitivity of an oscillation experiment to a given δm^2 depends on the L/E ratio, as illustrated in Fig. 1.

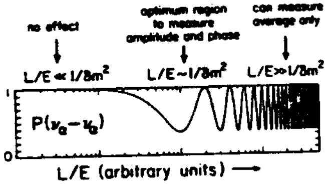

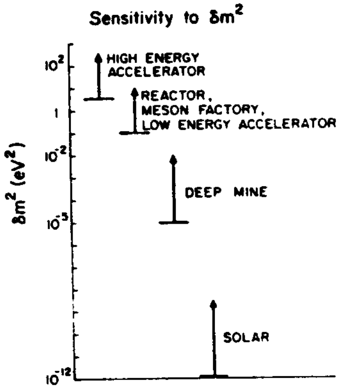

Fig. 1. Sensitivity of experiments to δm^2.

It is difficult to detect oscillation effects if $\Delta^2 \ll 1$. For instance, with $\delta m^2 \sim 1$ eV^2 and $\sin^2 2\alpha \sim \frac{1}{2}$, effects occur at the 10^{-2} level in accelerator experiments with $\frac{1}{2}\Delta \sim 0.04$ and at the 10^{-1} level in meson factory experiments with $\frac{1}{2}\Delta \sim 0.3$. With these mass and mixing scales, two-neutrino ν_e, ν_μ oscillations are on the borderline of admissibility[1] with present experimental limits.[2] Figure 2 shows the allowed and excluded regions of ν_e, ν_μ oscillation parameters, based on the Gargamelle $\nu_\mu \to \nu_e$ limit, which is the most stringent.

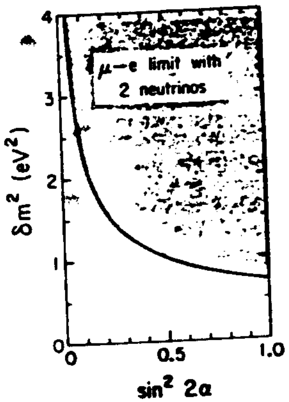

Fig. 2. Excluded region (shaded) of two neutrino oscillation parameters from experimental limit on $\nu_\mu \to \nu_e$ oscillations.

With three neutrinos, the accelerator and meson factory limits are even less constraining, because of the additional degrees of freedom in the mixing matrix; probability conservation no longer equates $P(e\to e)$ to $1 - P(e\to\mu)$, etc.

ACCELERATOR LIMITS

With n-neutrinos the leading oscillation (the first to occur as L/E increases from zero) has a simple form if one mass difference dominates, $\Delta_{in} \gg \Delta_{ij}$ for $i,j \neq n$. The transition probabilities for the leading oscillation are[3]

$$P(\alpha\to\alpha) = 1 - 4(|U_{\alpha n}|^2 - |U_{\alpha n}|^4)\sin^2\tfrac{1}{2}\Delta_{in}$$
$$P(\alpha\to\beta) = 4|U_{\alpha n}|^2\,|U_{\beta n}|^2\,\sin^2\tfrac{1}{2}\Delta_{in}\,. \qquad (7)$$

Note that an $\alpha\to\beta$ transition will be suppressed if $|U_{\beta n}|$ is small, independent of the value of $P(\alpha\to\alpha)$. For example, with three neutrinos, a small value of $|U_{\mu 3}|$ would suppress $P(e\to\mu)$ but allow $1 - P(e\to e)$ and $P(e\to\tau)$ to be large. Thus stringent limits on oscillations in any one off-diagonal channel do not preclude the existence of sizeable effects in other channels.

The leading oscillation for $n = 3$ can be parameterized by two mixing angles α and β by taking $|U_{e3}|^2 = \cos^2\alpha$, $|U_{\mu 3}|^2 = \sin^2\alpha\cos^2\beta$, and $|U_{\tau 3}|^2 = \sin^2\alpha\sin^2\beta$; this leads to[3]

$$P(e\to e) = 1 - \sin^2 2\alpha\,\sin^2\tfrac{1}{2}\Delta$$
$$P(e\to\mu) = \sin^2 2\alpha\,\cos^2\beta\,\sin^2\tfrac{1}{2}\Delta \qquad (8)$$
$$P(\mu\to\tau) = \sin^2 2\beta\,\sin^4\alpha\,\sin^2\tfrac{1}{2}\Delta\,.$$

Thus $\sin^2 2\alpha$ controls the amplitude of the $e\to e$ oscillation and $\cos^2\beta$ measures the relative amplitude for the $e\to\mu$ oscillation.

Present accelerator and meson factory limits[2,4-6] on oscillation probabilities are summarized in Fig. 3.

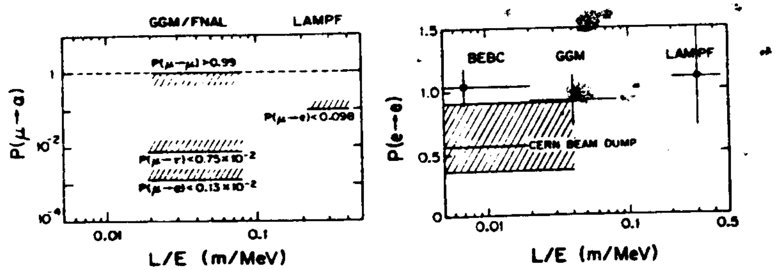

Fig. 3. Accelerator limits on neutrino oscillations.

Note that the BEBC ν_e flux measurement[5] of P(e→e) differs from the e→e probability inferred from the electron/muon ratio in the CERN beam dump bubble chamber result.[6] The constraints on leading oscillation parameters implied by the limits are shown in Fig. 4.

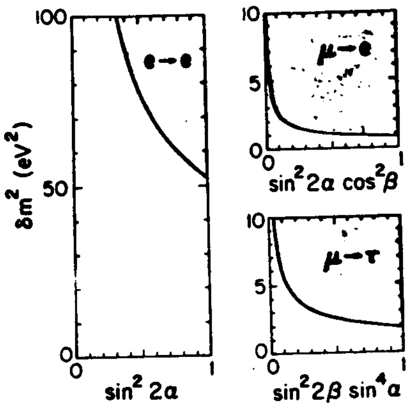

Fig. 4. Excluded regions (shaded) of the leading oscillation for three neutrinos.

A transition that is suppressed by mixing angles in the leading oscillation will in general occur at a non-suppressed level at higher L/E where the secondary mass differences enter. This is evident in the solution illustrated in Fig. 5 (solution A of Ref. 7), where the μ→e transition in the leading oscillation has been suppressed by a choice of small $U_{\mu 3}$. It is entirely possible that the μ→e transition could be highly suppressed at the meson factory L/E range and yet be very significant in deep mine L/E ranges.

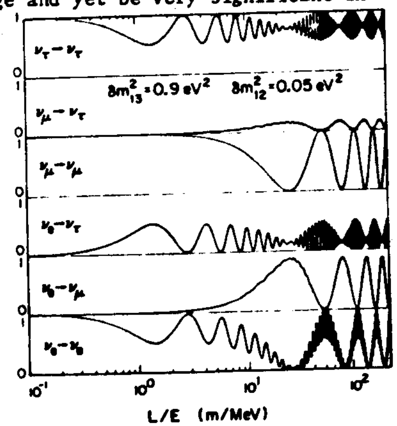

Fig. 5. Vacuum oscillations of a representative case.

CP VIOLATION

A direct measure of CP violation (CPV) in neutrino oscillations is the difference $P(\bar\alpha\to\bar\beta) - P(\alpha\to\beta)$ of $\bar\nu_\alpha \to \bar\nu_\beta$ and $\nu_\alpha \to \nu_\beta$ transition probabilities.[8] The equality $P(\alpha\to\beta) = P(\bar\beta\to\bar\alpha)$ is ensured by CPT invariance. CP-violating effects can be significant only in an L/E range where more than one mass difference plays a significant role; no CP-violating phases in the $U_{\alpha i}$ can be detected in the regime of the leading oscillation. For the three-neutrino case, the CPV difference is the same in all three channels:[9] $\nu_e \leftrightarrow \nu_\mu$, $\nu_e \leftrightarrow \nu_\tau$, $\nu_\mu \leftrightarrow \nu_\tau$. Figure 6 shows CP conjugate transition probabilities for a three-neutrino example (δm^2_{31} = 0.9 eV^2, δm^2_{21} = 0.05 eV^2 with Kobayashi-Maskawa angles θ_1 = 50°, $\theta_2 = \theta_3$ = 30° and CPV phase θ = 90°).

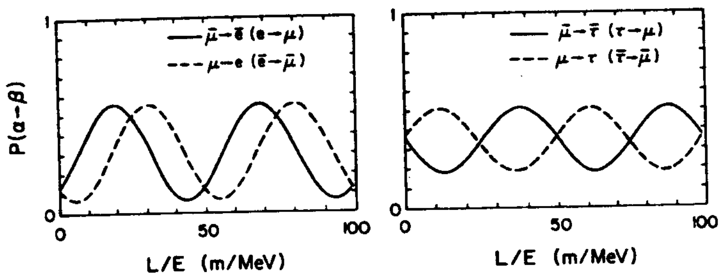

Fig. 6. Example of CP-violating splittings for three-neutrino oscillations.

The curves in Fig. 6 represent averages over the rapid oscillations associated with the larger mass difference. Even larger CP-violating effects are possible with δm^2 values that are more closely spaced. A proposed meson factory experiment could search for CPV effects in $\bar\nu_\mu \to \bar\nu_e$ and $\nu_\mu \to \nu_e$ channels.[10]

SOLAR NEUTRINOS

The observed ν_e flux from the sun is a factor of 0.3 ± 0.1 below that predicted by the standard solar model.[11] A possible explanation is the oscillation of ν_e neutrinos into other neutrino flavors.[12] Since $L/E \sim 10^{10}$ m/MeV for the ^{37}CL experiment, all δm^2 must be $\geq 0.5 \times 10^{-10}$ eV^2 to get sufficient ν_e flux depletion from oscillations. If all $\delta m^2 > 10^{-9}$ eV^2, the measurements are sensitive only to the average oscillation probability <P(e→e)>. The minimum value of <P(e→e)> attainable with oscillations of three neutrinos is 1/3, for all $|U_{ei}| = 1/\sqrt{3}$. For δm^2 in the range 10^{-9} - 10^{-10} eV^2, the spectrum averaged $\nu_e \to \nu_e$ transition probability can fall as low as 0.1 for either two-neutrino or three-neutrino mixing.[13]

REACTOR OBSERVATIONS

Using the inverse β-decay process $\bar{\nu}_e p \to e^+ n$, the reactor $\bar{\nu}_e$ flux has been measured at fixed distances L from the reactor core center. The ratio of the observed flux to the flux calculated from fissions gives a determination of $P(\bar{e}\to\bar{e})$. The principal uncertainty is the calculated flux, for which two recent versions have been given by Davis et al.[16] (DVMS) and Avignone-Greenwood[17] (AG). Measurements of the reactor e^- fission spectrum will resolve whether the calculated $\bar{\nu}_e$ spectra are correct, but there exists disagreement as to whether the issue has been settled yet.[18]

Figure 7 shows $P(\bar{e}\to\bar{e})$ deduced from the Reines et al. L = 11.2 m data and the Grenoble L = 8.7 m data, using the alternate choices of calculated flux. A leading oscillation with $\delta m^2 = 0.9\ eV^2$ and $\sin^2 2\alpha = 0.3$ or 0.5 is shown for comparison. The L = 11.2 m data suggest an oscillation effect of this scale; it is not evident whether a similar effect is present in the L = 8.7 m data.

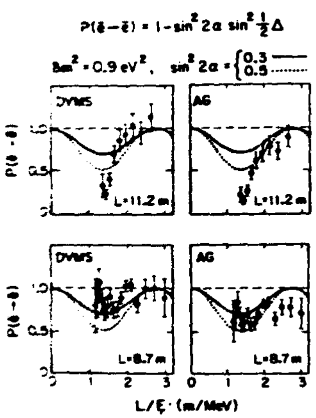

Fig. 7. Oscillation comparisons with reactor data for proton targets.

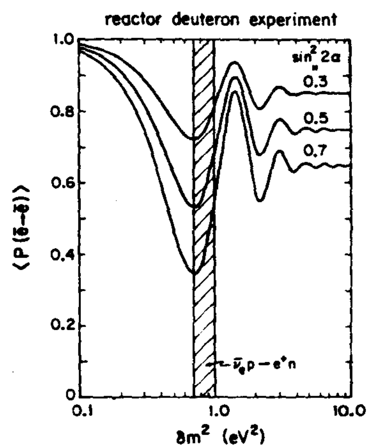

Fig. 8. Oscillation predictions for the reactor deuteron experiment.

The Irvine group has reported[19] indications of oscillations based on simultaneous measurements of charge-current and neutral current deuteron breakup reactions, $\bar{\nu}_e d \to nne^+$ and $\bar{\nu} d \to np\bar{\nu}$. Since the neutral current process is the same for all flavors of neutrino, it is immune to oscillations and provides a monitor of the initial $\bar{\nu}_e$ flux. The average probability for $\bar{\nu}_e$ oscillations can be extracted from

$$\bar{P}(\bar{e}\to\bar{e}) = \frac{[\bar{\sigma}(CC)/\bar{\sigma}(NC)]\text{experiment}}{[\bar{\sigma}(CC)/\bar{\sigma}(NC)]\text{theory at } L=0} \quad (9)$$

where $\bar{\sigma}$ denotes a spectrum averaged cross section. Variations in the theoretical ratio $\bar{\sigma}(CC)/\bar{\sigma}(NC)$ of up to 20% result from different final state interaction parameters.[20] The quoted experimental result for the DVMS spectrum of

$$\bar{P}(\bar{e}\to\bar{e}) = 0.40 \pm 0.22 \quad (10)$$

is based[21] on ^1S scattering lengths a(nn) = a(np) = -23.7 F and effective ranges $r_s(np)$ = 2.72 F, $r_s(nn)$ = 2.8 F. For the experimentally favored[22] values of a(nn) = -16.6 to -18.5 F, the transition probability becomes

$$\bar{P}(\bar{e}\to\bar{e}) = 0.43 \pm 0.24 . \quad (11)$$

Figure 8 shows a range of $\bar{P}(\bar{e}\to\bar{e})$ predictions for various leading oscillation parameters. The observed effect in the deuteron experiment is compatible with oscillation parameters that can describe the L = 11.2 m data.

DEEP MINE POSSIBILITIES

Deep mine experiments provide an opportunity to measure oscillations over baseline distances of 10 to 10^4 km, with δm^2 sensitivity down to $10^{-5}\ eV^2$. For energies 0.1 to 10^4 GeV the dominant neutrino sources are the $\pi(K) \to \mu\nu \to e\nu\nu\nu$ decay chains of charged pions and kaons which are produced in the atmosphere by cosmic radiation. The flux[23] is approximately $2(\nu_\mu + \bar{\nu}_\mu) + (\nu_e + \bar{\nu}_e)$, with some differences in the shapes of the energy distributions.

In experiments that detect muons from $\nu_\mu N \to \mu X$ interactions in the surrounding rock, ν_μ energies ranging from below 1 GeV up to 1 TeV are involved. From the ratio of observed to expected muon events, the combination $\langle P(\mu\to\mu)\rangle + \frac{1}{2}\langle P(e\to\mu)\rangle$ can be determined.

In proton decay experiments, electron and muon signals from neutrino interactions in a large water detector will come primarily from neutrinos with energies below 1 GeV. These experiments can measure the electron to muon ratio[24]

$$R(e/\mu) = \frac{N(e^\pm)}{N(\mu^\pm)} = \frac{\langle P(e\to e)\rangle + 2\langle P(\mu\to e)\rangle}{2\langle P(\mu\to\mu)\rangle + \langle P(e\to\mu)\rangle} \quad (12)$$

from upper or lower hemisphere ν_e, $\bar{\nu}_e$ and ν_μ, $\bar{\nu}_\mu$ events.

In both the above categories of deep mine experiments the neutrino energy is not determined and there is no $\nu/\bar{\nu}$ discrimination.

Vacuum oscillation effects can only become significant for neutrino energies

$$E(MeV) \lesssim L(m)\ \delta m^2(eV^2) \quad (13)$$

where L is the distance from source to detector and δm^2 is the largest vacuum mass-squared difference. For neutrinos which travel through 20% or more of the earth's radius there is the added complication of matter corrections[25,26] to vacuum oscillations. Due to coherent forward ν_e-e charged current scattering, the ν_e acquires an index of refraction n, given by

$$k(n-1) = \sqrt{2}\, G_F N_e \tag{14}$$

where N_e is the electron number density. The phase of the ν_e-part of the neutrino state is changed relative to the ν_μ, ν_τ parts by $e^{ik(n-1)x}$. The matter corrections enter for energies

$$E(\text{MeV}) \geq 5 \times 10^5\ \delta m^2(\text{eV}^2)\ , \tag{15}$$

with δm^2 the smallest vacuum mass-squared difference. The matter effects damp out $\nu_e \to \nu_\mu$ and $\nu_e \to \nu_\tau$ oscillations and $P(\nu_e \to \nu_e)$ approaches unity for energies

(16)

$$E(\text{MeV}) \geq 5 \times 10^6\ \delta m^2(\text{eV}^2)\ . \tag{16}$$

The onset of matter effects and the subsequent quenching of ν_e oscillations occur successively for each δm^2 as E increases above the lower limits in Eqs. (15) and (16), respectively. Figure 9 graphically outlines these regions.

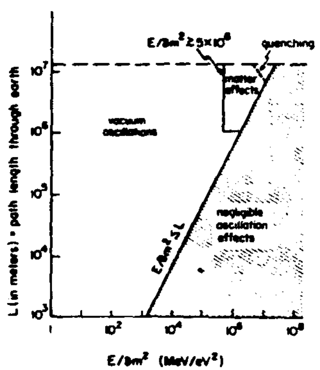

Fig. 9. Oscillation ranges for deep mine experiments.

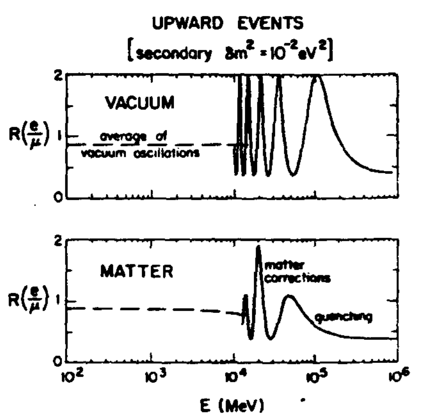

Fig. 10. Example of electron to muon event ratio in deep mine experiments for neutrinos through earth's center.

The sensitivity to vacuum and matter oscillations of past, present, and future deep mine experiments is summarized in the following table.

Experiments	L and E Ranges	δm^2 Sensitivity for Vacuum Oscillations	δm^2 Sensitivity for Matter Oscillations
Case-Irvine-Witwatersrand and Kolar gold field $(\nu_\mu, \bar{\nu}_\mu)$	$10^4 \leq L \leq 5\times10^5$ m $10^2 \leq E \leq 10^6$ MeV	$\geq 10^{-2}$ eV^2	None (L too short)
Baksan, Homestake, and proton decay $(\nu_\mu, \bar{\nu}_\mu)$	$L \leq 1.3\times10^7$ m $10^2 \leq E \leq 10^6$ MeV	$\geq 10^{-4}$ eV^2	10^{-4} - 1 eV^2
Proton decay $(\nu_\mu, \bar{\nu}_\mu; \nu_e, \bar{\nu}_e)$	$L \leq 1.3\times10^7$ m $10^2 \leq E \leq 10^3$ MeV	$\geq 10^{-5}$ eV^2	10^{-5} - 10^{-3} eV^2

Figure 10 illustrates vacuum and matter oscillation $R(e/\mu)$ results for direct upward neutrinos, based on vacuum oscillation parameters $\delta m^2_{31} = 0.9$ eV^2, $\delta m^2_{21} = 10^{-2}$ eV^2, $\theta_1 = 50°$, $\theta_2 = 20°$, $\theta_3 = 30°$, $\delta = 0$. The solid curves are averages of the rapid oscillations associated with the larger δm^2. In the absence of oscillations, $R(e/\mu) = \frac{1}{2}$. The qualitative aspects of these results scale in $E/\delta m^2$. Hence for a secondary mass scale of $\delta m^2_{31} = 10^{-4}$ eV^2, the matter corrections would enter around E = 100 MeV. The prospects for deep mine studies of oscillations appear reasonable given appropriate δm^2 scales and appreciable $e \to \mu$ mixing.

ACKNOWLEDGMENTS

I am indebted to Kerry Whisnant for valuable assistance in the preparation of this review and to Roger Phillips and Sandip Pakvasa for discussions. The contributions of my collaborators are gratefully acknowledged.

This research was supported in part by the University of Wisconsin Research Committee with funds granted by the Wisconsin Alumni Research Foundation, and in part by the Department of Energy under contract DE-AC02 76ER00881-183.

REFERENCES

1. V. Barger, K. Whisnant, D. Cline and R.J.N. Phillips, J. Phys. G6, L165 (1980).
2. J. Blietschau et al., Nucl. Phys. B133, 205 (1978); S. E. Willis et al., Phys. Rev. Lett. 44, 522 (1980).
3. V. Barger, K. Whisnant and R.J.N. Phillips, Phys. Rev. D22, 1636 (1980).
4. B. Roe, private communication; T. Kondo, in these proceedings.
5. H. Deden et al., CERN/EP 80-164.
6. P. Fritze et al., Oxford preprint 71/80.
7. V. Barger, K. Whisnant, D. Cline and R.J.N. Phillips, Phys. Lett. 93B, 194 (1980).
8. N. Cabibbo, Phys. Lett. 72B, 333 (1978).
9. V. Barger, K. Whisnant and R.J.N. Phillips, UW-Madison DOE-ER/00881-177 (1980).
10. T. Bowles, T. Dombeck and R. Burman, LAMPF proposal 638 (1980).
11. J. Bahcall and R. Davis, Jr., in these proceedings.
12. V. N. Gribov and B. Pontecorvo, Phys. Lett. 28B, 493 (1979); J. N. Bahcall and S. C. Frautschi, Phys. Lett. 29B, 623 (1979).
13. V. Barger, K. Whisnant and R.J.N. Phillips, DOE-ER/00881-179 (1980).
14. H. W. Sobel, F. Reines and E. Pasierb, Univ. Cal.-Irvine report 48 (1980).
15. F. Boehm et al., Phys. Lett. 97B, 310 (1980).
16. B. R. Davis et al., Phys. Rev. C19, 2259 (1979).
17. F. T. Avignone and Z. D. Greenwood, Univ. of South Carolina report (1980).
18. P. Vogel, in these proceedings; F. Avignone, private communication.
19. F. Reines, H. W. Sobel and E. Pasierb, Phys. Rev. Lett. 45, 1307 (1980).
20. A. Dar, Technion preprint (1980).
21. A. Soni, private communication.
22. B. Kühn, F. Z. Elem. Chastits At. Yachra 6, 347 (1975) [Sov. J. Part. Nucl. 6, 139 (1976)]; J. C. Alder et al., Helv. Phys. Acta 51, 90 (1978); B. Gabioud et al., Phys. Rev. Lett. 42, 1508 (1979).
23. J. L. Osborne, S. S. Said and A. W. Wolfendale, Proc. Phys. Soc. (London) 86, 93 (1965); E.C.M. Young, Cosmic Rays at Ground Level, Institute of Physics Press, p. 105, A. W. Wolfendale, ed., London and Bristol (1973).
24. B. Cortez and L. R. Sulak in Proc. Erice Workshop on Grand Unification (1980); J. Losecco, in these proceedings.
25. L. Wolfenstein, Phys. Rev. D17, 2369 (1978).
26. V. Barger, K. Whisnant, S. Pakvasa and R.J.N. Phillips, DOE-ER/00881-152 (1980).

IMPLICATIONS OF THE CERN BEAM DUMP PROGRAM RELATING TO NEUTRINO OSCILLATIONS

Don D. Reeder
University of Wisconsin, Madison, WI 53706

ABSTRACT

The underlying concept of a beam dump experiment is that the neutrinos which arise from ordinary long lived particles are suppressed relative to those which are produced by short lived parents by interacting the parents in a dense medium before they decay. The arrangement at the CERN Laboratory in Geneva, Switzerland is shown schematically in Figure 1. The "prompt" component of the ν flux is produced by the decay of the new hadrons (charm, top, bottom, etc.). The "non-prompt" component is produced by ordinary long lived pions, kaons and hyperons which decay before interaction despite a large dense absorber.

A serendipitous coincidence resulted in the beam dump/target being located far from the detectors (820 m to 910 m as shown in Figure 1). Thus the (1.27 L/E) figure for the experiment which is

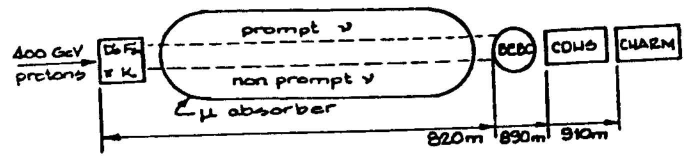

Figure 1) Schematic diagram of the CERN Beam Dump experiment.

the paramount parameter for neutrino oscillation tests is .05-.01. I will use the by-now-familiar notation which relates the probability of a neutrino produced as type 1 and interacting as type 2 to mixing parameter $\sin^2 2\theta$ and the difference in mass-squared Δ.

$$P(\nu_1 \to \nu_2) = |\delta_{12} - \sin^2 2\theta \sin^2 (\frac{1.27\Delta L}{E})|$$

where $\Delta = |m_1^2 - m_2^2|$ in eV^2

L = drift distance in m, E = energy of neutrino in MeV

The extraction of the prompt ν flux is done in two ways. The direct experimental procedure is to measure the neutrino flux using dump/targets of differing density. As shown in Figure 2 when extrapolated to infinite density (zero absorption length) the "prompt" ν flux is identified. Alternatively, the "non-prompt" contribution can be calculated using knowledge of π, K production spectra, geometry, etc. The prompt component is the remainder after subtraction of this calculated background flux.